EXPERIMENTAL METHODS FOR SPALLING MONITORING DURING AND AFTER FIRE TESTS

Francesco Lo Monte and Roberto Felicetti

Department of Civil and Environmental Engineering, Politecnico di Milano, Milan (Italy)

Abstract

Monitoring the progress of spalling and moisture front in concrete elements subjected to heating is a challenging task, since most of the available techniques can be hardly implemented in the test furnace. This is a critical issue, because the measurement of temperature and pressure can be not sufficient to define the conditions for spalling if depth and area involved, as well as occurrence time are not known.

Generally speaking, monitoring can be performed by means of Real-Time or Post-Event survey. As concerns the former approach, promising results are expected to come from ultrasonic Pulse-Echo and Ground-Penetrating Radar methods, both based on the measurement of the time delay of (ultrasonic and electromagnetic, respectively) echoes reflected by the specimen side exposed to fire. Other methods for Real-Time monitoring can be Digital Image Processing of pictures taken during heating, and Acoustic Emission.

As regards spalling survey after fire, laser profilometry, optical size measurement and weighing of the collected splinters can be co-ordinately used to depict some statistical trends of the fracture process due to fire.

These methods (except Acoustic Emission) have been – or will be – implemented in the case of fire tests performed on concrete slabs subjected to heating at the bottom face, and the results are discussed in the present paper.

Keywords

Digital Image Processing, laser profilometry, ultrasonic Pulse-Echo, optical size measurement, spalling monitoring.

1. INTRODUCTION

Explosive spalling is the violent expulsion of chunks from the exposed face of concrete members when subjected to heating. Such phenomenon is hard to be fully understood, due to the presence of different influencing factors (heating rate, concrete thermo-physical properties, initial moisture content and saturation level) and parameters (pore pressure and stress) [1-4]. Moreover, in order to well define the conditions of spalling initiation and propagation, the onset and the progression of the detachments should be monitored.

This last aspect is very interesting and represents a challenging issue. The quantification of spalling time, depth and extension during a fire is, in fact, difficult, since most of the available techniques can be hardly implemented in the test furnace.

The investigations herein considered can be divided in Real-Time and Post-Event survey. In the former case the measurements are performed during heating, while the latter methods are based on observations after cooling down. The approaches based on ultrasonic Pulse-Echo, Ground-Penetrating Radar and on Digital Image Processing belong to the first set, while laser profilometry, and optical size measurement and weighing of the collected splinters belong to the second one. It is worth noting that other Real-Time survey approaches can be find in the literature, such as the Acoustic Emission–AE, which proved to be rather interesting even though to distinguish micro- and macro-cracking from spalling is very difficult [5,6].

The above-discussed techniques (except AE) have been considered within a research project in progress at the Politecnico di Milano (Milan, Italy) in collaboration with CTG-Italcementi Group (Bergamo, Italy) [7]. The experimental campaign consists in spalling tests performed on concrete slabs (800x800x100 mm) subjected to heating at the intrados according to the Standard Fire curve, under biaxial membrane loading (mean compressive stress of 10 MPa). Slabs are uniformly heated at the bottom face by means of a propane burner, while load is applied via 8 hydraulic jacks restrained by a steel frame (Fig.1). A total of 4 concrete mixes have been designed ($f_c \geq 60$ MPa; calcareous aggregate) and 2 slabs per mix have been cast. The mixes differ only for fibre addition: no fibre (1), 40 kg/m^3 of steel fibre (2), and 2 kg/m^3 of monofilament (3) or fibrillated (4) polypropylene fibre.

The abovementioned Real-Time survey techniques are implemented during the tests at the cold face, where the low temperature allows to use the instrumentation. Only Digital Image Processing can directly monitor the hot face, since it consists in pictures taken on the exposed intrados through a small window on the lateral wall of the furnace.

The different approaches and results are shown in the following.

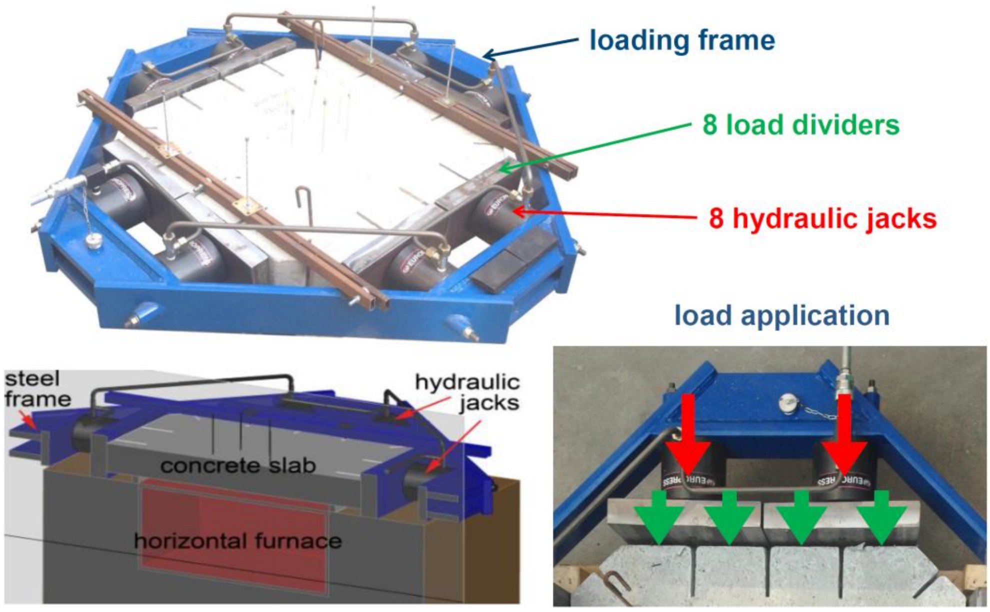

Figure 1: Spalling test performed on concrete slabs subjected to Standard Fire at the intrados under biaxial membrane loading. Heat is applied via a horizontal furnace with a propane burner, while biaxial load is obtained by means of a welded steel frame restraining 8 hydraulic jacks.

2. REAL-TIME SURVEY

2.1 Ultrasonic Pulse-Echo method

Ultrasonic Pulse-Echo is based on the reflection-time evaluation of ultrasonic pulses propagating through the thickness of an element [8] (see Fig.2a). If an ultrasonic emitter is applied to the surface of a member, the elastic waves propagate in the continuum without reflection/refraction if no discontinuity or change in acoustic impedance is crossed.

When a discontinuity (such as the sudden variation of material properties, or the interface between two layers) is met, elastic waves are partially refracted and partially reflected, depending on the variation magnitude of acoustic impedance (the higher the stiffness, the higher the acoustic impedance). If reflection occurs due to a decrease of impedance, the amplitude sign reverses.

A special case occurs when discontinuity is represented by air, since the reflection is practically total and the reversal in the wave amplitude is observed (negligible or nil air stiffness for compression or shear elastic waves, respectively). This is the reason why, such method proves to be effective in detecting delaminations and voids in concrete members [9,10]. The ultrasonic source can be a mechanical impact of small hammers or metallic balls (namely, Impact-Echo) or pulses produced by ultrasonic transducers (namely, ultrasonic Pulse-Echo) [11]. Post-processing of data can be performed in the frequencies framework through the Fourier Transform, this approach requiring to eliminate "parasitic" effect caused by the global excitation of the specimen and by edge-effects [12], or in the time-domain by evaluating the reflection time as described in the following.

In the present case, the shear pulse emitter/receiver A1220 by Acoustic Control Systems was used (Fig.2b). Between the ultrasonic device and the concrete slab extrados, an insulation stone brick was interposed in order to keep the temperature low while guarantying the contact. The presence of the brick was obviously taken into account in data post-processing, reflections occurring also at the concrete-to-stone interface.

In Fig.3a the typical ultrasonic waves observed at the receiver are shown as a function of fire duration. The coloured dots indicate the different reflections. The green dot represents the first measured ultrasonic wave that was reflected at the stone-to-concrete interface. The violet dot indicates the second wave that was reflected three times inside the stone, while the orange dot highlights the wave reflected at the concrete-to-air interface. It is worth noting that in correspondence of violet and orange dots there was a change of amplitude sign since one reflection occurred between a stiff material (concrete or stone) and air.

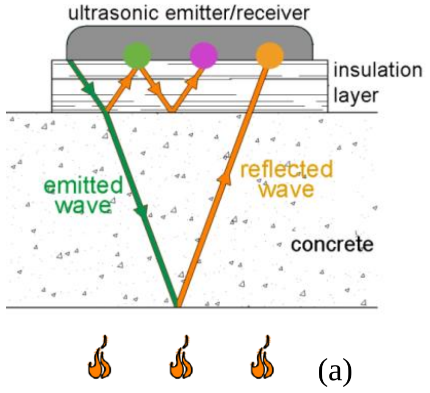

(a)


(b)

Figure 2: (a) Pulse-Echo principle and (b) adopted ultrasonic device placed on the slab.

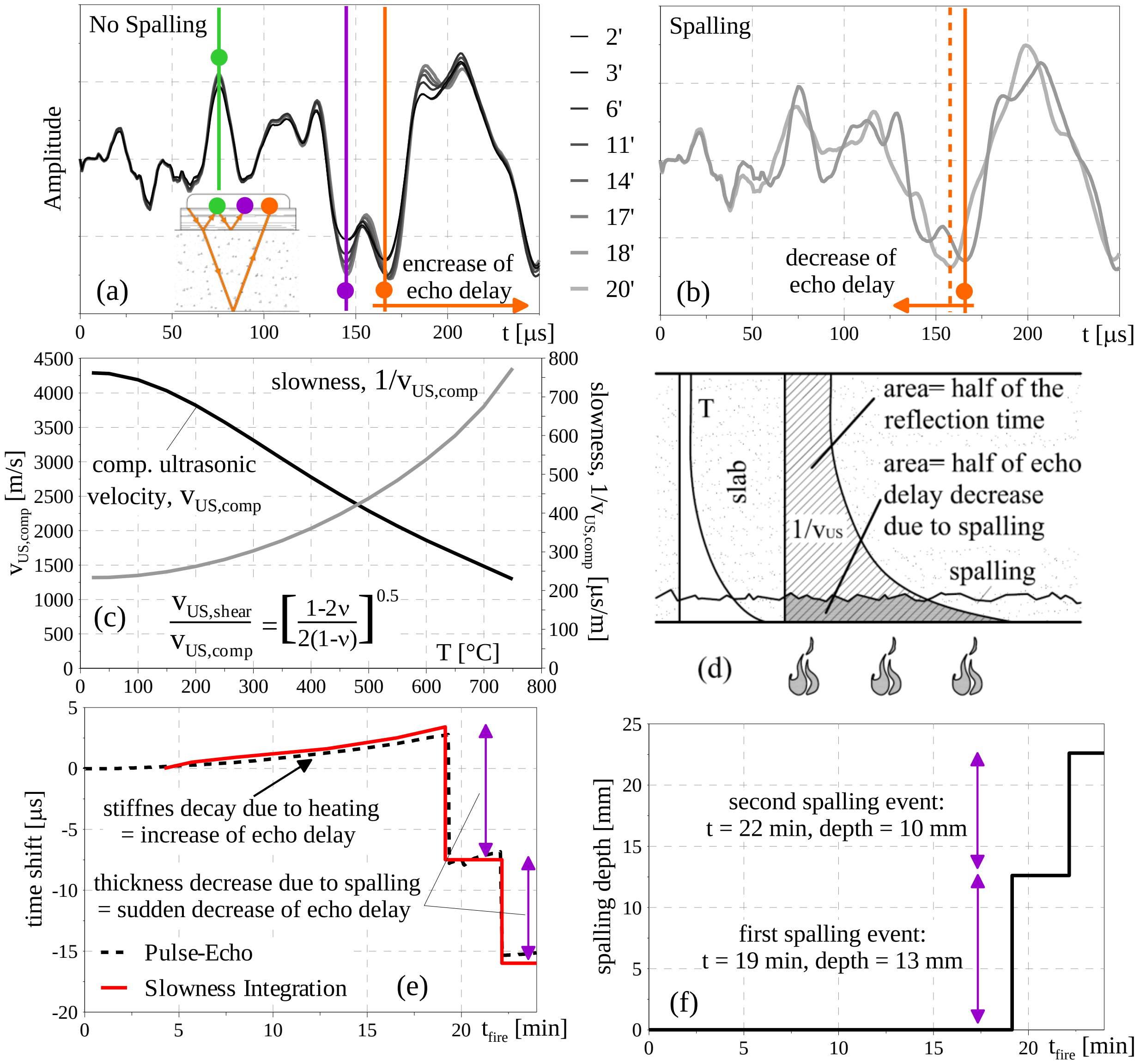

Figure 3: Ultrasonic Pulse-Echo method: ultrasonic waves at the receiver for different fire durations showing (a) the echo delay increase due to heating and (b) the sudden decrease due to spalling; (c) ultrasonic velocity of compression waves as a function of temperature; (d) slowness integration principle; (e) plot of time delay obtained via both ultrasonic Pulse-Echo and slowness integration; and (f) computed spalling depth with time.

During heating, the decay of the mechanical properties of concrete makes the ultrasonic waves slower, this resulting in a delay in the reflection time at the slab intrados (orange dot). On the opposite, the reflection times in stone (green and violet dots) are almost constant, the temperature remaining close to ambient (Fig.3a).

When spalling occurs, a sudden decrease in concrete thickness takes place and the time of reflection instantaneously decreases (Fig.3b). Such sudden decrease is considered to compute the spalling depth.

The reflection time, in fact, can be evaluated by post-processing once the temperatures within concrete and the decay of ultrasonic wave velocity due to heating are known.

In the case at hand, the thermal field was known thanks to the continuous measurements of temperature at 6 different slab depths during heating, while the decay of the compression ultrasonic wave velocity with temperature was evaluated in a previous experimental campaign conducted on the same concrete mixes (Fig.3c). Thus, the shear ultrasonic wave velocity and, hence, the slowness (inverse of velocity) could be evaluated along the depth.

The reflection time was computed by integrating the slowness through the depth (see Fig.3d). In correspondence of spalling, the thickness reduction in the slab necessary to match the time shift (or echo delay) highlighted by the Pulse-Echo measurement could, therefore, be computed. Such thickness reduction corresponds to the spalled layer (Fig.3d).

The reflection time as a function of fire duration was, hence, evaluated by integration and taking into account the thickness reduction due to spalling. The outcome is reported in Fig.3e together with the reflection time measured by ultrasonic Pulse-Echo.

In Fig.3f the obtained spalled thickness is depicted as a function of time. The first event occurred at 19.3 min of heating with a spalling depth of 13 mm, while the second took place after 22 min with a thickness of 10 mm.

2.2 Digital Image Processing

Digital Image Processing is another viable method to implement during the test. By comparing two frames taken by a video camera right before and after a spalling event, the extent of the detached fragment can be assessed as shown in Fig.4, where the blue area represents the region in which differences between two consecutive pictures appear due to the detachments. This technique is still under development, but it shows to be very interesting thanks to its simplicity and effectiveness in providing information about the area involved in the different spalling events.

It is important to observe, however, that no information is given about spalling depth. This drawback could be partially overcome if the weight of the specimen is continuously monitored during the test. In this way, in fact, knowing the area of the spalled region and its weight a reliable indication about fragment average thickness could be worked out.

2.3 Ground-Penetrating Radar – GPR

Ground-Penetrating Radar (GPR) is a non-destructive technique based on the study of the propagation through a material or a fluid of electromagnetic waves. whose velocity depends mainly on the dielectric properties of the host means [13,14].

The material properties governing electromagnetic wave velocity is the dielectric constant, which is defined as the ratio between the electric permittivity of the material at hand and of air. It is worth noting that air and water have very low and very high dielectric constant, respectively, so making dielectric properties of concrete strongly influenced by air and moisture contents [15,16].

In particular, water content has a two-fold effect, since it leads to an increase in both the polarization mechanism and the real permittivity (with an increase of the dielectric constant even more than two times going from dry to saturated concrete [17]). The former effect induces a decrease of the electromagnetic energy, hence to a reduction on reflected-wave amplitude peaks [18-20], while the latter causes a delay of the reflection time (because of travel time increase). Thanks to theses aspects, good results in monitoring water content and saturation in concrete have been shown in the literature, as reported in [17,21,22].

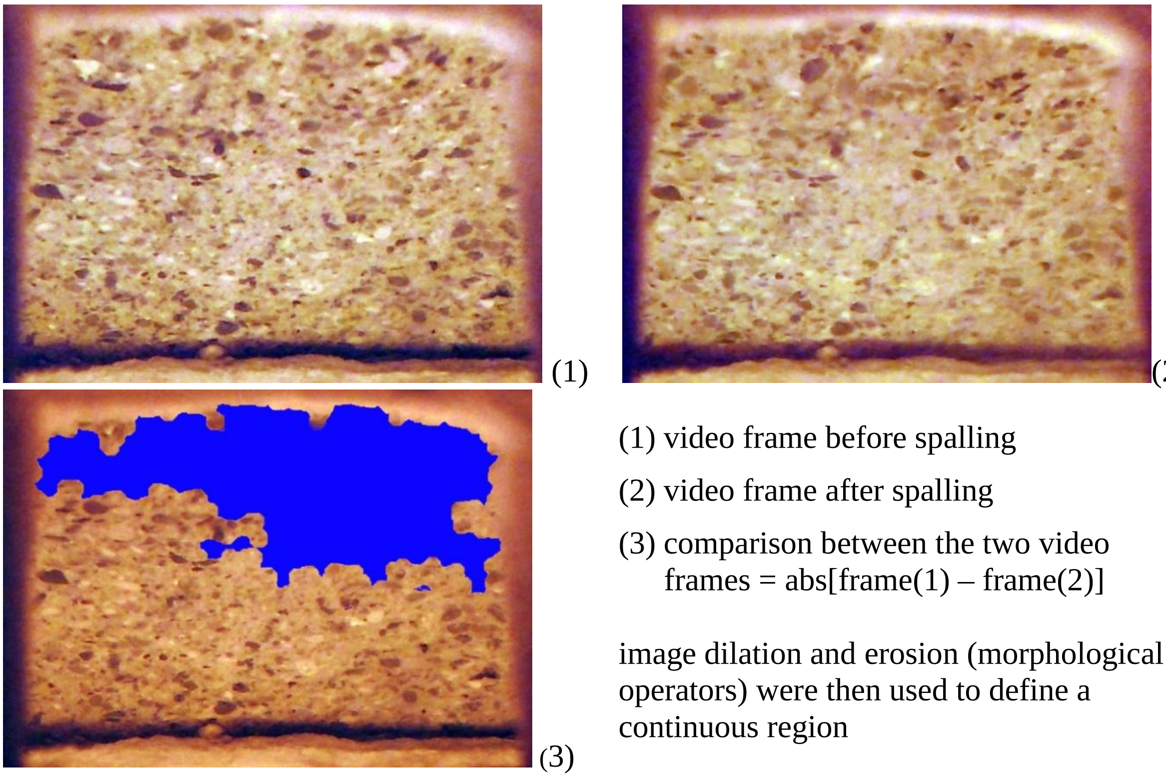

(1) (2) (3)

(1) video frame before spalling

(2) video frame after spalling

(3) comparison between the two video frames = abs[frame(1) – frame(2)]

image dilation and erosion (morphological operators) were then used to define a continuous region

Figure 4: Comparison of two video frames preceding and following a spalling event.

Similarly to the ultrasonic pulses, electromagnetic waves propagating through a continuum are partly reflected and partly refracted when a sudden change in electric properties is met. The travel time of reflected waves can be used to evaluate layer thicknesses or defect depths, as already discussed for ultrasonic Pulse-Echo.

This technique is still under study and it is expected to give information about spalling depth and moisture front. It will be implemented only in the next tests, and, so far, no results are available for the experimental campaign herein presented.

3. POST-EVENT SURVEY

3.1 Laser profilometry

Important indication about spalling was also provided by measuring the spalled profile after cooling down. In the case at issue, a laser profilometer was used.

The maximum depth of the spalled layer turned out to be 60 mm (namely, 60% of the initial thickness!), while the average value was 43 mm. The average value was evaluated considering the whole heated area and it was affected by the rounded edges. Looking at the section depicted in Fig.5c, however, it is clear that the spalling surface was rather homogeneous.

This consideration is very important, because it means that in uniform conditions of heating and loading, explosive spalling seems mainly driven by pressure and stress gradients along the depth.

In Fig.5, the slab appears divided in four big pieces, since at the end of heating, two orthogonal through-thickness cracks formed.

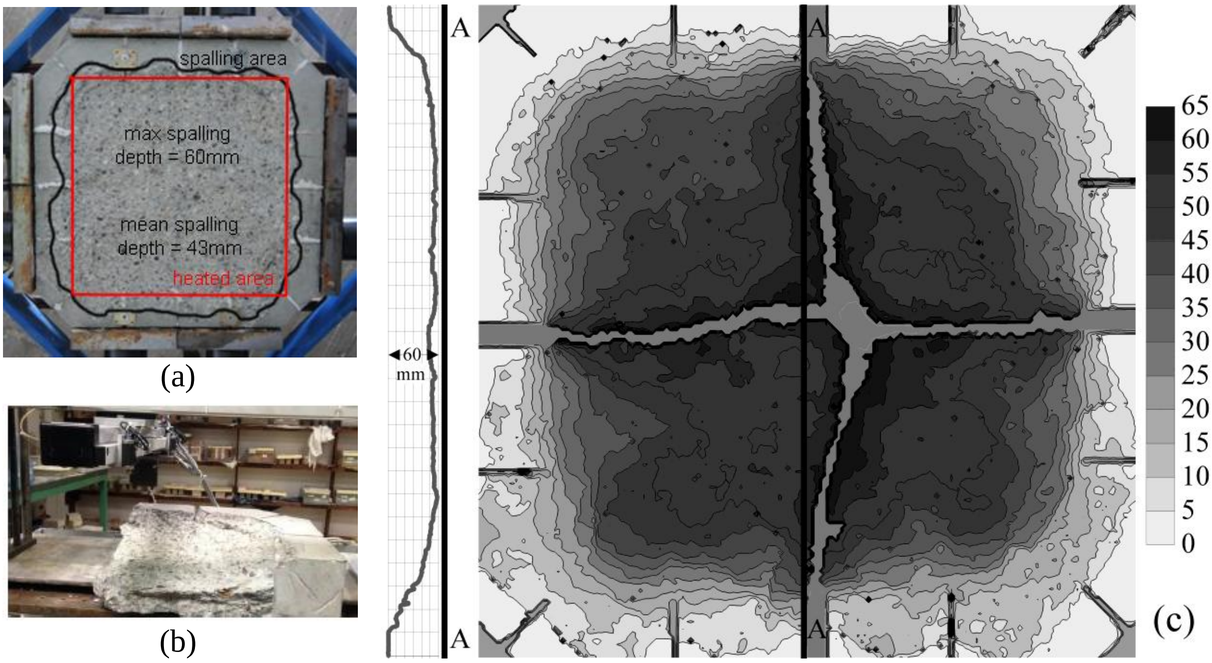

Figure 5: Laser profilometry: (a) spalled slab, (c) adopted device and (c) contour lines of spalling surface.

3.2 Optical size measurement and weighing of splinters

Investigation on the splinters collected at the end of the fire can help in describing spalling development, in addition to Real-Time survey techniques such as ultrasonic Pulse-Echo.

After cooling down, all the chunks of concrete were weighed, so to evaluate their volume on the basis of the known concrete density.

Afterwards, different pictures of all the pieces placed on white paper sheets were taken as shown in Fig.6a. The images were then post-processed via Binary Large OBject – BLOB Analysis (see Fig.6b) and the surface area of each splinter was computed by means of MATLAB. Hence, the average thickness of each spalled concrete piece was evaluated simply dividing the volume by the surface area.

It was possible to discern the debris belonging to the intrados from those of the internal part of the slab, since the former ones were characterized by a smooth surface (bottom surface during casting). This information was very important, allowing to distinguish the average thickness in the first severe spalling event from the following progressive detachments.

The obtained average thicknesses are shown in Fig.6c for each splinter. It is worth noting that the mean values of the average thicknesses of the splinters were evaluated by weighed average, on the basis of splinters area, so to give more relevance to the greater fragments.

The total area of the debris coming from the intrados was 0.30 m^2, namely 84% of the heated area (= 0.6x0.6 = 0.36 m^2). The total weight of the collected chunks was 7.9 kg, while the weight of the remaining dust gathered from the furnace was 26.2 kg. Thus, the collected volume was about 0.016 m^3, with an average thickness of the spalled layer equal to 45 mm (in the heated area of 0.6x0.6 m), in very good agreement with the average thickness given by the laser profilometry.

In Fig.6d the probability distribution of the average thicknesses is shown, referring to splinters area and separating the data relative to the intrados (first event) from the others.

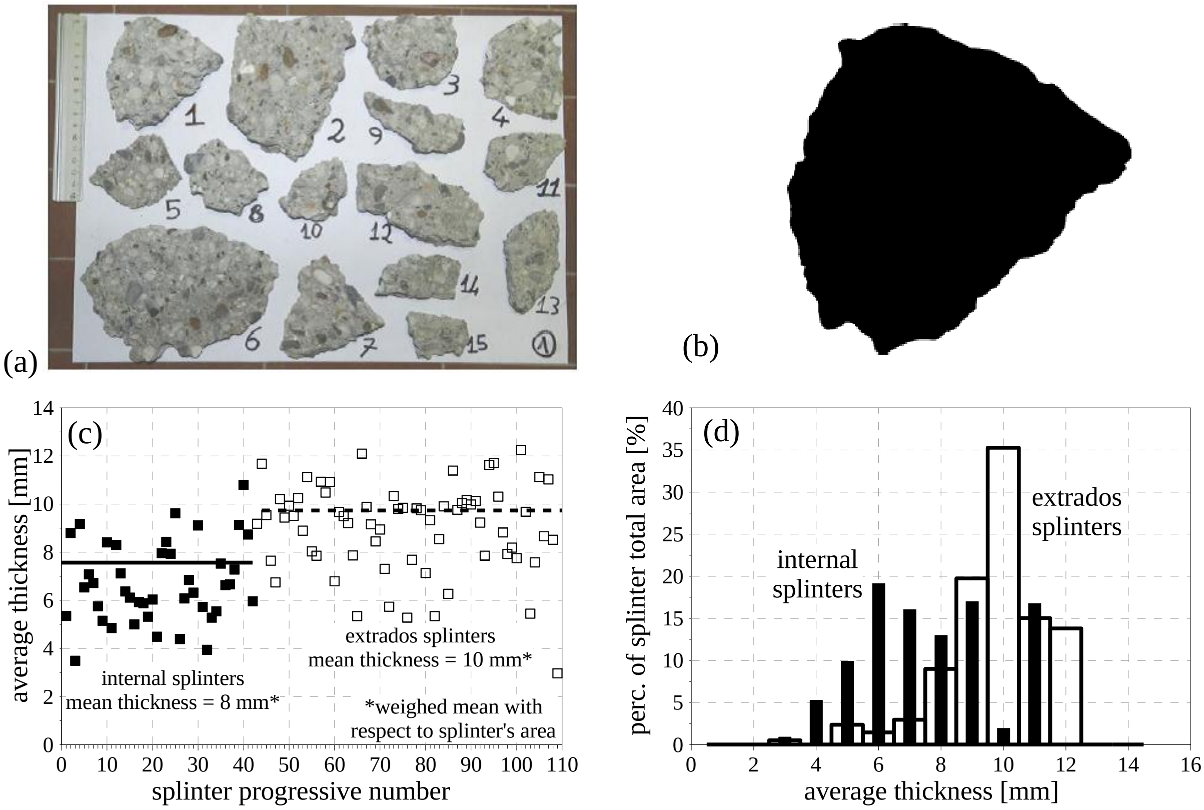

Figure 6: Optical size measurement and weighing of splinters: (a) splinters placed on a white paper sheet, (b) filtered black and white image of a splinter (BLOB); (c) average splinters thickness and mean values, and (d) probability distribution.

As shown, the average thickness is 10 and 8 mm, for the first and the following events, respectively. Considering that the thickness on the edges of each chunk was smaller than in the central part, the effective depth of the spalled layers could be greater. Hence, the obtained result can be considered in very good agreement with the outcome of the ultrasonic Pulse-Echo measurements (13 and 10 mm for the first and the following events, respectively).

This technique proves to be interesting in corroborating the information given by other methods, but has the drawback of providing no indication about spalling time.

4. COMBINED APPROACH

As above-discussed, a few rather simply yet effective methods can be implemented in fire tests for Real-Time and/or Post-Event survey. Table 1 shows as each method proves to have advantages and drawbacks, demonstrating to hardly provide by itself all the needed data.

This is the reason why, the combination of at least two approaches is strongly recommended, this becoming a way to monitor all the main important parameters, such as spalling time and depth, as well as area involved in the detachments.

Among the possible alternatives, Digital Image Processing and ultrasonic Pulse-Echo can represent the best combination, allowing to measure spalling time, depth and extension.

Regarding Post-Event methods, optical size measurement of splinters revealed to be rather interesting, since it gives indication about spalling depth and extensions.

Table 1: information provided by survey methods (RT = Real-Time, PE = Post-Event).

** to be studied* *^ final outcome only*		Information provided			
		Spalling time	Spalling depth	Spalling extension	Moisture front
Ultrasonic Pulse-Echo	RT	yes	yes	no	*
Digital Image Processing	RT	yes	no	yes	no
Ground-Penetrating Radar	RT	*	*	*	*
Laser profilometry	PE	no	yes^	yes^	no
Optical size measurement of splinters	PE	no	yes	no	no

5. CONCLUSIONS

A recent experimental investigation was launched at the Politecnico di Milano in Collaboration with CTG Italcementi Group on concrete spalling sensitivity, based on testing concrete slabs heated according to Standard Fire curve at the intrados, while subjected to membrane biaxial loading. Within this project, different methods to monitor concrete spalling during and after heating (Real-Time and Post-Event survey, respectively) have been – or will be – implemented. Among the first group ultrasonic Pulse-Echo, Ground-Penetrating Radar and Digital Image Processing have been studied, while among the second set laser profilometry and optical size measurement and weighing of splinters have been considered.

All the measurements proved to be rather easy to be performed, while effective in providing useful information. Generally speaking, however, none of the methods seemed to be able to give by itself all the needed data, such as spalling time, thickness and extension. On the other hand, the combined implementation of two or more of the above-discussed techniques can give a comprehensive picture of the development of such phenomenon.

AKNOWLEDGMENTS

The Authors are grateful to CTG-Italcementi Group (Bergamo, Italy) for the design of the concrete mixes and the useful contribution in preparing the specimens. Fondazione Lombardi Ingegneria (Minusio, Switzerland) is also thanked for the financial support given to this research project.

REFERENCES

[1] Kalifa P., Menneteau F. D. & Quenard D. ‘Spalling and pore pressure in HPC at high temperatures’, *Cement and Concrete Research* 30 (2000) 1915–1927.

[2] Khoury A. G. ‘Effect of fire on concrete and concrete structures’, *Progress in Structural Engineering and Materials* 2 (2000) 429–447.

[3] Khoury G.A. ‘Polypropylene Fibres in Heated Concrete. Part 2: Pressure Relief Mechanisms and Modelling Criteria’, *Magazine of Concrete Research* 60 (3) (2008) 189–204.

[4] Yufang F. and Lianchong L., ‘Study on mechanism of thermal spalling in concrete exposed to elevated temperatures’, *Materials and Structures* 44 (2010) 361–376.

[5] Grosse C., Richter R., Ozbolt J., Dehn F. and Juknat M., ‘Spalling of HPC Evaluated by Acoustic Emission and Numerical Analysis’, *Proceedings of the 2nd International RILEM Workshop on Concrete Spalling due to Fire Exposure*, 5-7 October, Delft (the Netherlands) (2011) 157–163.

[6] Pereira F., Pistol K., Korzen M., Weise F., Pimienta P., Carré H. and Huismann S., ‘Monotoring of Fire Damage Processes in Concrete by Pore Pressure and Acoustic Emission Measurements’, *Proceedings of the 2nd International RILEM Workshop on Concrete Spalling due to Fire Exposure,* 5-7 October, Delft (the Netherlands) (2011) 69–77.

[7] Lo Monte F. and Felicetti R., ‘Spalling Test on Concrete Slabs under Biaxial Membrane Loading’, *Proceedings of the 4th International Workshop on Concrete Spalling due to Fire Exposure,* 8-9 October, Leipzig (Germany) (2015).

[8] Carino N. J., ‘The Impact-Echo Method: an Overview*’, Proceedings of the 2001 Structures Congress & Exposition*, May 21-23 2001,Washington, D.C., American Society of Civil Engineers, Reston, Virginia, Peter C. Chang, Editor, 2001. 18 p.

[9] Cheng C. and Sansalone M., ‘The impact-echo response of concrete plates containing de-laminations: numerical, experimental and field studies*’, Mat. and Struct.* 26 (1993) 274–285.

[10] Lin Y., Sansalone M., and Carino N.J. ‘Finite Element Studies of the Impact-Echo Response of Plates Containing Thin Layers and Voids*’, J. of Nondestructive Evaluation* 9 (1) (1990) 27–47.

[11] Krause M., Barmann M., Frielinghaus R., Kretzschmsr F., Kroggel O., Langenberg K. L., Maierhofer C., Muller W., Neisecke J., Schickert M., Schmitz V., Wiggenhauser H. and Wollbold F., ‘Comparison of pulse-echo methods for testing concrete’, *NDT&E International* 30 (4) (1997) 195–204.

[12] Sansalone M., and Carino N.J. ‚Transient Impact Response of Thick Circular Plates*’, Journal of Research of the National Bureau of Standards* 92 (6) (1987) 355–367.

[13] Maierhofer C., ‘Non destructive evaluation of concrete infrastructure with ground penetrating radar’, *ASCE J Mater Civil Eng* 15 (3) (2003) 287–97.

[14] Yehia S., Qaddoumi N., Farrag S. and Hamzeh L., ‘Investigation of concrete mix variations and environmental conditions on defect detection ability using GPR’, *NDT&E International* 65 (2014) 35–46.

[15] Sbartai Z. M. , Laurens S.,Balayssac J. P., Ballivy G. and Arliguie G. ‘Effect of concrete moisture on radar signal amplitude’, *ACI Mater Journal* 103 (6) (2006).

[16] Lai W. L., Kou S. C., Tsang W. F. and Poon C. S., ‘Characterization of concrete properties from dielectric properties using ground penetrating radar*’, Cem. and Conc. Res.* 39(8) (2009) 687–695.

[17] Laurens S., Balayssac J. P., Rhazi J., Klysz G. and Arliguie, ‘Non-destructive evaluation of concrete moisture by GPR: experimental study and direct modeling’, *Materials and Structures* 38 (2005) 827–832

[18] Sbartai Z. M., Laurens S., Balayssac J. P., Arliguie G. and Ballivy G., ‘Ability of the direct wave of radar ground-coupled antenna for NDT of concrete structures’, *NDT&E International* 39 (5) (2006) 400–407,2006.

[19] Klys G. and Balayssac J. P., ‘Determination of volumetric water content of concrete using ground-penetrating radar’, *Cement and Concrete Research* 37 (2007) 1164–1171.

[20] Laurens S., Balayssac J. P, Rhazi J. and Arliguie G., ‘Influence of concrete relative humidity on the amplitude of Ground-Penetrating Radar (GPR) signal’, *Materials and Structures* 35 (2002) 198–203.

[21] Sbartai Z. M., Breysse D., Larget M. and Balayssac J. P., ‘Combining NDT techniques for improved evaluation of concrete properties, *Cem. & Conc. Comp.* 34 (2012) 725–733.

[22] Rodriguez-Abad, Martinez-Sala R., Mene J., ‘Water penetrability in hardened concrete by GPR’ *Proceedings of 15th International Conference on Ground Penetrating Radar - GPR 2014,* June 30-July 4 (2014) 862–867.